J|A|C|S
ARTICLES
Published on Web 05/10/2007

Selective Hydrogenation of the C═O Bond in Acrolein through the Architecture of Bimetallic Surface Structures

Luis E. Murillo,[†] Amit M. Goda,[‡] and Jingguang G. Chen*,[‡]

Contribution from the Departments of Materials Science and Engineering and of Chemical Engineering, Center for Catalytic Science and Technology, University of Delaware, Newark, Delaware 19716

Received January 12, 2007; E-mail: jgchen@udel.edu

Abstract: In the current study we have performed experimental studies and density functional theory (DFT) modeling to investigate the selective hydrogenation of the C═O bond in acrolein on two bimetallic surface structures, the subsurface Pt−Ni−Pt(111) and surface Ni−Pt−Pt(111). We have observed *for the first time* the production of the desirable unsaturated alcohol (2-propenol) on Pt−Ni−Pt(111) under ultra-high vacuum conditions. Furthermore, our DFT modeling revealed a general trend in the binding energy and bonding configuration of acrolein with the surface d-band center of Pt−Ni−Pt(111), Ni−Pt−Pt(111), and Pt(111), suggesting the possibility of using the value of the surface d-band center as a parameter to predict other bimetallic surfaces for the selective hydrogenation of acrolein.

Introduction

In this paper we report the selective hydrogenation of acrolein (CH_2═CHCH═O) to produce 2-propenol (CH_2═$CHCH_2OH$), which represents *for the first time* the hydrogenation of the C═O bond in acrolein on bimetallic surfaces under ultra-high vacuum (UHV) conditions. The selective hydrogenation of α,β-unsaturated aldehydes to unsaturated alcohols is of growing interest for the production of fine chemicals and pharmaceutical precursors.[1,2] In addition, a fundamental understanding of the competitive hydrogenation mechanisms of the C═C and C═O bonds in unsaturated aldehydes offers the opportunity to identify, and potentially design, catalyst formulations and structures for the selective hydrogenation of organic molecules containing multiple functional groups. Experimental efforts for the hydrogenation of unsaturated aldehydes have been primarily focused on supported catalysts of group VIII transition metals, in particular platinum-based bimetallic catalysts.[1−3] Due to the polycrystalline nature of the supported catalysts, a fundamental understanding of the hydrogenation pathways is lacking at present. Zaera et al. have attempted to determine the reaction pathways of acrolein, the smallest α,β-unsaturated aldehyde, on the single crystal surface of Pt(111) under UHV conditions.[4,5] Although novel decomposition pathways were observed on Pt(111), the hydrogenation of either the C═O or C═C bond was not detected.[5] More recently, density functional theory (DFT) modeling has been performed on the adsorption and reaction of acrolein on Pt(111).[6,7] These studies suggested that the absence of gas-phase 2-propenol was likely due to its strong bonding on the Pt(111) surface.

In principle, hydrogenation pathways can be selectively modified by the formation of bimetallic surfaces on Pt(111), in particular by controlling the structures of the bimetallic surfaces.[8−12] For instance, depositing one monolayer (ML) of Ni on Pt(111) can lead to the formation of either the Ni−Pt−Pt(111) surface structure, with Ni atoms residing on the topmost surface, or the Pt−Ni−Pt(111) subsurface structure, with most Ni atoms residing between the first and second layers of Pt, as described previously.[11] These structures have been previously confirmed using low-energy ion scattering (LEIS) and grazing-angle X-ray photoelectron spectroscopy (XPS).[11] These two bimetallic surfaces have very unique electronic and chemical properties as compared to Pt(111). For example, results from DFT modeling revealed that the surface d-band center of the subsurface Pt−Ni−Pt(111) was further away from the Fermi level as compared to those of both Pt(111) and Ni−Pt−Pt(111) surfaces,[13,14] leading to weaker binding energies of atomic hydrogen and alkenes on Pt−Ni−Pt(111). The weaker binding energies in turn led to a novel low-temperature hydrogenation pathway of alkenes on Pt−Ni−Pt(111), as confirmed experi-

[†] Department of Materials Science and Engineering.
[‡] Department of Chemical Engineering.

(1) Gallezot, P.; Richard, D. *Catal. Rev.—Sci. Eng.* **1998**, *40*, 81 and references therein.
(2) Claus, P. *Top. Catal.* **1998**, *5*, 51 and references therein.
(3) Maki-Arvela, P.; Hajek, J.; Salmi, T.; Murzin, D. Y. *Appl. Catal., A* **2005**, *292*, 1 and references therein.
(4) de Jesus, J. C.; Zaera, F. *Surf. Sci.* **1999**, *430*, 99.
(5) de Jesus, J. C.; Zaera, F. *J. Mol. Catal. A* **1999**, *138*, 237.
(6) Loffreda, D.; Delbecq, F.; Fabienne, V.; Sautet, P. *Angew. Chem., Int. Ed.* **2005**, *44*, 5279.
(7) Loffreda, D.; Delbecq, F.; Fabienne, V.; Sautet, P. *J. Am. Chem. Soc.* **2006**, *128*, 1316.
(8) Beccat, P.; Bertolini, J. C.; Gauthier, Y.; Massardier, J.; Ruiz, P. *J. Catal.* **1990**, *126*, 451.
(9) Jerdev, D. I.; Olivas, A.; Koel, B. E. *J. Catal.* **2002**, *205*, 278.
(10) Hwu, H. H.; Eng, J., Jr.; Chen, J. G. *J. Am. Chem. Soc.* **2002**, *124*, 702.
(11) Kitchin, J. R.; Khan, N. A.; Barteau, M. A.; Chen, J. G.; Yakshinksiy, B.; Madey, T. E. *Surf. Sci.* **2003**, *544*, 295.
(12) Olivas, A.; Jerdev, D. I.; Koel, B. E. *J. Catal.* **2004**, *222*, 285.
(13) Skoplyak, O.; Barteau, M. A.; Chen, J. G. *J. Phys. Chem. B* **2006**, *110*, 1686.
(14) Kitchin, J. R.; Nørskov, J. K.; Barteau, M. A.; Chen, J. G. *J. Chem. Phys.* **2004**, *120*, 10240.

10.1021/ja070264m CCC: $37.00

mentally.[10] In addition, studies on other bimetallic systems, such as Fe[8] and Sn[15] on Pt(111), also demonstrated novel hydrogenation pathways of β-substituted acrolein, including crotonaldehyde and 3-methylcrotonaldehyde. It was observed that the hydrogenation activity was enhanced by the formation of bimetallic surfaces.

In the current study we have performed experimental studies and DFT modeling to explore whether the unique chemical properties of the Pt−Ni−Pt(111) subsurface structure, such as the weaker binding energies of atomic hydrogen and alkenes, would lead to the *selective hydrogenation* of the C═O bond in acrolein. The formation of the desirable hydrogenation product, 2-propenol, was detected from the Pt−Ni−Pt(111) subsurface structure using temperature programmed desorption (TPD). Parallel surface vibrational studies provided evidence of the interaction of the C═O bond of acrolein with Pt−Ni−Pt(111), most likely responsible for the selective hydrogenation of the C═O bond on this surface. Furthermore, DFT modeling confirmed that one of the adsorption configurations of acrolein occurred via the interaction of the C═O bond with Pt−Ni−Pt-(111), which was not favored on either Ni−Pt−Pt(111) or Pt-(111). The DFT results also showed a correlation between the adsorption energy and bonding configuration of acrolein with the surface d-band center, which demonstrated the possibility to potentially predict, on the basis of the value of the d-band center, other desirable bimetallic structures for the selective hydrogenation of the C═O bond in acrolein.

Experimental and Modeling Methods

The surface science experiments were performed in a UHV chamber equipped with capabilities for TPD and high-resolution electron energy loss spectroscopy (HREELS). The bimetallic surfaces were prepared by depositing Ni onto a Pt(111) single crystal (Metal Crystals and Oxides, Ltd., Cambridge, U.K.). The Ni−Pt−Pt(111) surface structure and the Pt−Ni−Pt(111) subsurface structure were obtained by depositing one monolayer of Ni at 300 and 600 K, respectively.[11] TPD experiments were performed at a heating rate of 3 K/s. Absolute TPD yields were estimated using the procedure developed by Ko et al.,[16] correcting for mass spectrometer sensitivity factors and using experimental fragmentation patterns. The integrated area of the CO desorption spectrum was used as a base for the absolute yield calculation. The absolute yield of CO at saturation coverage was calculated experimentally by comparing it with the expected saturation coverage on Pt(111) (0.68 ML);[17] the yields of all the desorption species were calculated by using the corresponding sensitivity factors relative to CO.

The HREEL spectra were collected with a primary beam energy of 6 eV. In the case of on-specular measurements, the angles of incidence and reflection were 60° with respect to the surface normal. For the off-specular measurements, a reflection angle of 50° with respect to the surface normal was used. Count rates in the elastic peak were in the range of 3×10^4 to 3×10^5 counts per second (cps), and the spectral resolution was between 30 and 40 cm^{-1} full width at half-maximum (fwhm). The sample was annealed to the specified temperature with a linear rate of 3 K/s, held for 5 s, and then cooled to ~100 K for data collection.

Self-consistent periodic slab calculations were carried out on the basis of the gradient-corrected DFT method. All calculations were performed using periodic density functional theory as implemented in the code VASP (Vienna ab initio Simulation Package).[18] The Kohn−Sham equations were solved using a plane-wave basis set with a cutoff energy of 396 eV. The PW91 functional was used to describe the exchange correlation term. The core electrons and the nuclei of the atoms were described by the Vanderbilt ultrasoft pseudopotential.[19,20] Electronic energies were calculated using a $3 \times 3 \times 1$ *k*-point grid mesh. The coadsorption of acrolein and atomic hydrogen was studied using 3×3 supercells, with nine metal atoms in each layer and with two hydrogen atoms and one acrolein molecule adsorbed per unit cell. Four metal layers were used, with the top two layers allowed to relax in each case. A vacuum region equivalent in thickness to six metal layers was used to separate the slabs to avoid any electronic interactions between them. Calculations for gas-phase acrolein and adsorbate−metal systems were carried out spin-unpolarized. The value of the surface d-band center was calculated as the first moment of the projected d-band density of states on the surface atoms with reference to the Fermi level.

Results and Discussion

Figure 1 compares the TPD results following the hydrogenation of 0.5 langmuir (1 langmuir = 1×10^{-6} Torr·s) of acrolein on Pt−Ni−Pt(111), Ni−Pt−Pt(111), and Pt(111), after the coadsorption of acrolein and atomic hydrogen on these surfaces at 100 K. Figure 1 displays the TPD spectra of mass 31 amu, a cracking fragment for both CH_2═$CHCH_2OH$ (2-propenol) and $CH_3CH_2CH_2OH$ (1-propanol), masses 58 and 57 amu, cracking fragments for both CH_2═$CHCH_2OH$ and CH_3CH_2CH═O (propanal), and mass 60 amu, a cracking fragment of $CH_3CH_2CH_2OH$. The production of either CH_2═$CHCH_2OH$ or $CH_3CH_2CH_2OH$ is not detected from Pt(111) and Ni−Pt−Pt(111), as indicated by the absence of any desorption peaks in the 31 and 60 amu TPD spectra from the two surfaces. In contrast, a relatively intense desorption peak is observed at 260 K from the Pt−Ni−Pt(111) subsurface structure and is attributed to the formation of primarily 2-propenol, on the basis of the peak intensity ratio in the 31 and 60 amu spectra.

The formation of propanal, from the hydrogenation of the C═C bond in acrolein, from the 57 and 58 amu TPD spectra, shows a relatively weak peak from the Pt(111) surface at 192 K. The detection of desorption peaks at 215, 254, and 302 K in the 57 and 58 amu spectra on the Ni−Pt−Pt(111) surface, coupled with the absence of desorption peaks in the 31 amu TPD, suggests the formation of propanal. In addition, the peak area ratios of the individual peaks between masses 57 and 58 amu are similar to the ones found for the intensity ratios of the same masses in the mass spectrum of propanal ($area_{58}/area_{57} \approx 3$). On the Pt−Ni−Pt(111) surface, the peaks at 184 and 215 K in the 57 and 58 amu spectra are attributed to the desorption of propanal, while the peak at 260 K is from the contribution from both propanal and 2-propenol on the basis of the comparison with the 31 amu spectrum.

The yields for the three gas-phase hydrogenation products, 2-propenol, propanal, and 1-propanol, are shown in Table 1. The yields were quantified from the TPD peak areas from the three surfaces. The empirical procedure developed by Ko et al.[16] for the correction of mass spectrometer sensitivity factors of these yield calculations is used. Peak deconvolution is performed when the desorption feature is due to the

(15) Jerdev, D. I.; Koel, B. E. *Surf. Sci.* **2002**, *513*, L391.
(16) Ko, E. I.; Benziger, J. B.; Madix, R. J. *J. Catal.* **1980**, *62*, 264.
(17) Ertl, G.; Neumann, M.; Streit, K. M. *Surf. Sci.* **1977**, *64*, 393.
(18) (a) Kresse, G.; Hafner, J. *Phys. Rev. B* **1993**, *47*, 558. (b) Kresse, G.; Furthmuller, J. *Comput. Mat. Sci.* **1996**, *6*, 15. (c) Kresse, G.; Furthmuller, J. *Phys. Rev. B* **1996**, *54*, 11169.
(19) Vanderbilt, D. *Phys. Rev. B* **1990**, *41*, 7892.
(20) Kresse, G.; Hafner, J. *J. Phys.: Condens. Matter* **1994**, *6*, 8245.

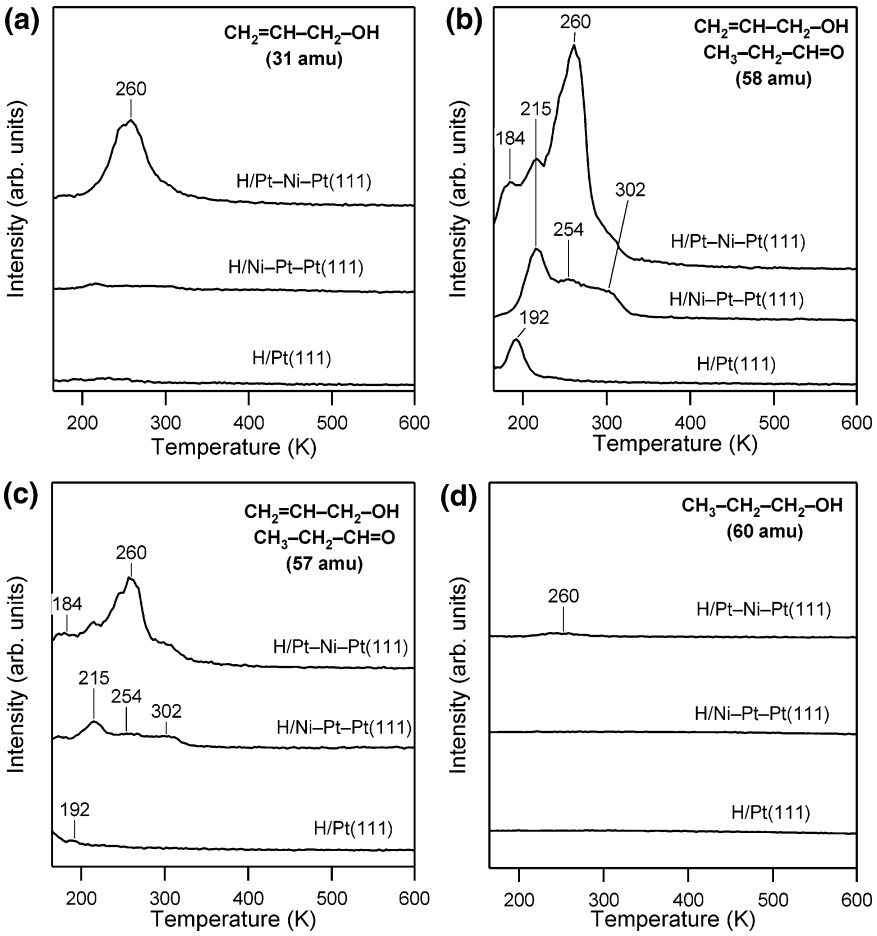

Figure 1. TPD spectra following the reaction of acrolein with coadsorbed atomic hydrogen at 100 K on different surfaces: (a) 2-propenol (31 amu), (b, c) propanal and 2-propenol (58 and 57 amu, respectively), and (d) 1-propanol (60 amu).

Table 1. TPD Yields (Molecules per Surface Pt Atom) of Hydrogenation Products after the Reaction of 0.5 langmuir of Acrolein with Preadsorbed Atomic Hydrogen on Different Surfaces

surface	propanal (CH_3CH_2CH═O)	2-propenol (CH_2═CH_2CH_2OH)	1-propanol ($CH_3CH_2CH_2OH$)
H/Pt(111)	0.004	0	0
H/Ni−Pt−Pt(111)	0.025	0	0
H/Pt−Ni−Pt(111)	0.12	0.025	0.002

contribution of the cracking patterns of the mixed products, such as the desorption peaks at 260 K on the H/Pt−Ni−Pt(111) surface. Overall, the TPD results indicate that the hydrogenation of the C═O bond does not occur on either Pt(111) or Ni−Pt−Pt(111). In contrast, the subsurface Pt−Ni−Pt(111) is active for the hydrogenation of acrolein to produce both CH_2═$CHCH_2$-OH and CH_3CH_2CH═O.

To further understand the onset of the novel C═O hydrogenation pathway on the Pt−Ni−Pt(111) surface, the bonding configurations of acrolein have been investigated using HREELS, which is an ideal technique to differentiate between the various bonding configurations of acrolein. For example, Figure 2 shows HREEL spectra following the coadsorption of acrolein and atomic hydrogen on the two bimetallic structures, subsurface Pt−Ni−Pt(111) and surface Ni−Pt−Pt(111), after the annealing to 200 K, which is below the desorption temperature of the hydrogenation products. The physisorbed spectrum of acrolein, after multilayer adsorption on Pt(111), is also included at the bottom of Figure 2 for comparison with the vibrational frequencies listed at the top of the figure. These frequencies are the calculated gas-phase values of acrolein using Gaussian 03.[21] At 100 K (not shown), the frequencies of adsorbed acrolein on H/Pt−Ni−Pt(111) are very similar to the corresponding gas-phase values, suggesting weakly bonded acrolein on this bimetallic surface. After annealing to 200 K, the ν(C═O) mode at ∼1700 cm^{-1} disappears from the subsurface Pt−Ni−Pt(111), indicating either the formation of di-σ-bonded acrolein through the C−O moiety or the onset of the hydrogenation of the C═O bond. However, the absence of the ν(O−H) mode, even in the off-specular spectrum, suggests that the C═O hydrogenation does not occur on the surface at 200 K. The remaining ν(C═C) mode at ∼1569 cm^{-1} is characteristic of the ν(C═C) stretching mode in the gas-phase spectrum of 2-propenol. The corresponding off-specular spectrum shows vibrational features similar to those described in the on-specular mode. In contrast, the nature of the surface intermediate on H/Ni−Pt−Pt(111) is significantly different. For example, the ν(C═O) mode remains on the H/Ni−Pt−Pt(111) surface at 200 K, indicating that the C═O bond of acrolein does not interact strongly with the surface, which should be most likely responsible for the lack of C═O hydrogenation on Ni−Pt−Pt(111), as confirmed in the TPD measurements.

To correlate the TPD results in Figure 1 and Table 1 and the vibrational fingerprints observed in HREELS with the adsorption

(21) Frisch, M. J.; et al. *Gaussian 03, revision B.04*; Gaussian, Inc.: Pittsburgh, PA, 2003.

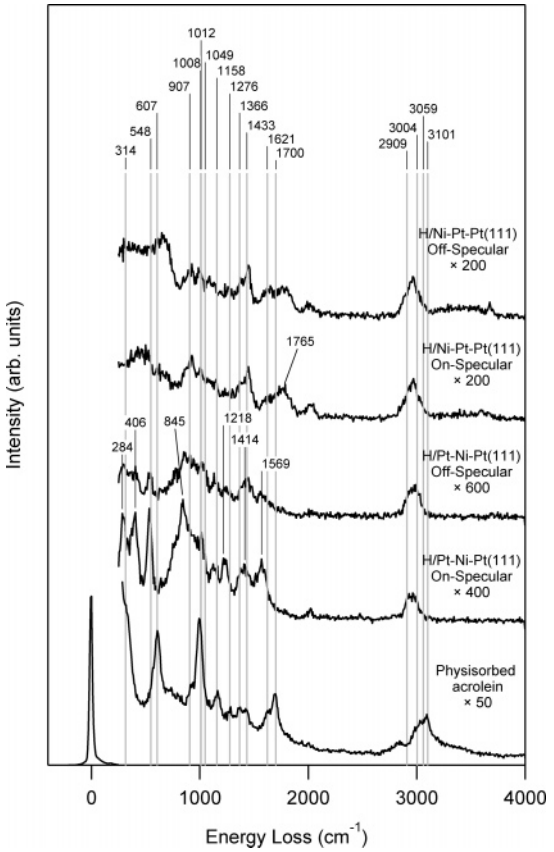

Figure 2. On and off-specular HREEL spectra of the coadsorption of acrolein and atomic hydrogen on H/Pt−Ni−Pt(111) and H/Ni−Pt−Pt(111) surfaces after annealing to 200 K. Physisorbed acrolein at 100 K (bottom spectrum) and the calculated gas-phase vibrational features are included for comparison.

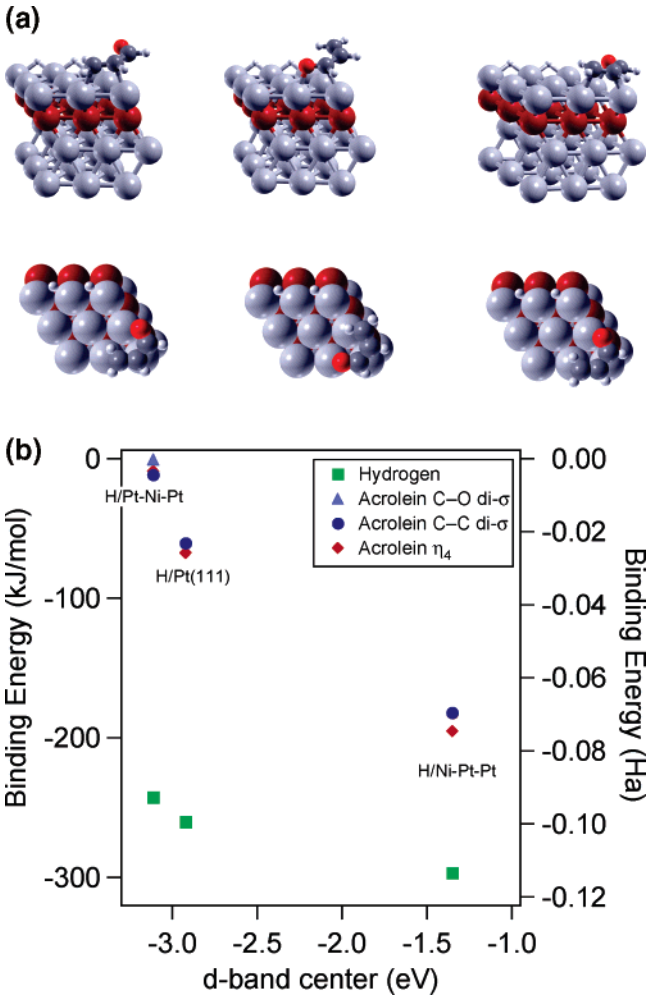

Figure 3. (a) Side view and top view of configurations of adsorbed acrolein through di-σ-C−C, di-σ-C−O, and η_4(C,C,C,O) on the Pt−Ni−Pt(111) surface. (b) DFT calculations of acrolein and hydrogen binding energies vs the surface d-band center for H/Pt−Ni−Pt(111), H/Pt(111), and H/Ni−Pt−Pt(111) surfaces.

configurations of acrolein, we have performed DFT modeling to determine the binding energies (BEs) of different adsorption configurations of acrolein on H/Pt−Ni−Pt(111), H/Ni−Pt−Pt-(111), and H/Pt(111) surfaces. Figure 3a displays the three binding configurations of acrolein on the Pt−Ni−Pt(111) surface through di-σ-C−C, di-σ-C−O, and η_4(C,C,C,O). Figure 3b shows the self-consistent periodic DFT calculations for atomic hydrogen and acrolein bonded in the di-σ-C−C, di-σ-C−O, and η_4(C,C,C,O) configurations. The DFT results show that the BE values of acrolein are in the order H/Pt−Ni−Pt(111) < H/Pt-(111) < H/Ni−Pt−Pt(111), which follows a trend similar to that of the BE values of atomic hydrogen on these surfaces. In addition, on all three surfaces the di-σ-bonding through the C−C bond of acrolein is stronger than through the C−O bond. In fact, on the H/Pt(111) and H/Ni−Pt−Pt(111) surfaces, the binding through the di-σ-C−O configuration is so weak that it converts to the flat η_4(C,C,C,O) configuration during the course of the DFT calculations. Hence, on H/Pt(111) and H/Ni−Pt−Pt(111) surfaces acrolein tends to be adsorbed through either the di-σ-C−C or the η_4(C,C,C,O) mode. Last, the η_4(C,C,C,O) configuration shows a binding energy similar to that of the di-σ-C−C configuration on all the surfaces. By comparing the trends in the TPD results in Table 1 and DFT modeling in Figure 3b, it appears that the higher hydrogenation activity on H/Pt−Ni−Pt(111) is related to the weaker bonding of both acrolein and atomic hydrogen, which is consistent with our previous studies of correlating the presence of weakly bonded alkenes and weakly bonded atomic hydrogen with enhanced hydrogenation activity of alkenes.[10] The onset of the selective hydrogenation pathway on H/Pt−Ni−Pt(111) is most likely due to the similar BE values of the three adsorption configurations of acrolein. The similar binding energies would lead to the adsorption of acrolein through both the C═O and C═C moieties, making it possible to hydrogenate both the C═O and C═C bonds, as summarized in the hydrogenation activities in Table 1. On the other hand, as predicted by DFT, the adsorption of acrolein on H/Pt(111) and H/Ni−Pt−Pt(111) surfaces does not occur through the di-σ-C−O configuration, hence making it difficult to hydrogenate the C═O bond, as confirmed by the absence of the 2-propenol product in the TPD measurements.

It should be pointed out that DFT modeling is often inadequate in describing weakly adsorbed species, such as acrolein on H/Pt−Ni−Pt(111), as indicated by the weak binding energies. Other types of modeling approaches, such as those that can more accurately describe dispersive van der Waals interactions, should be performed to quantitatively differentiate the three adsorption configurations on the H/Pt−Ni−Pt(111) surface. A more accurate prediction of the hydrogenation selectivity should also include the calculations of the activation barriers for the different reaction pathways. However, these calculations are computationally much more expensive than the

DFT modeling of binding energies, such as those shown in Figure 3. Overall, the comparison of the trend in the binding energies in Figure 3 suggests that the onset of the selective hydrogenation pathway of the C═O bond on Pt−Ni−Pt(111) is most likely related to the following two factors: (1) the weaker binding energies of acrolein and atomic hydrogen, which should favor the hydrogenation and subsequent desorption of the reaction products from the surface, and (2) the smaller difference between the binding energies of the three bonding configurations, which should enhance the possibility of bonding through the C═O moiety and therefore the subsequent hydrogenation of the C═O bond. Assuming that both factors are related to the selective hydrogenation of the C═O bond, and assuming that the correlation of binding energies with the surface d-band center continues in Figure 3b for other surfaces, one can predict that bimetallic surfaces with the d-band center further away from the Fermi level might have higher selectivity than Pt−Ni−Pt(111). From our previous DFT calculations,[14,22] the surface d-band center of the Pt−3d−Pt(111) subsurface structure shifts away from the Fermi level as the subsurface 3d metal moves toward the left-hand side of the periodic table. If the trend in Figure 3b continues for other Pt−3d−Pt(111) surfaces as the subsurface 3d metal moves from Ni to Ti, the binding through the C═O bond of acrolein could potentially become preferred, making those Pt−3d−Pt(111) surfaces more selective toward the C═O bond hydrogenation. However, it is also important to keep in mind that, as the surface d-band center moves further away from the Fermi level, the bonding of acrolein might become too weak for the subsequent hydrogenation to occur. Experimental and DFT studies are under way to extend the correlation in Table 1 and Figure 3b by investigating the binding energies and hydrogenation selectivity of acrolein on the subsurface structures of other Pt−3d−Pt(111) bimetallic surfaces.

(22) Menning, C. A.; Hwu, H. H.; Chen, J. G. *J. Phys. Chem. B* **2006**, *110*, 15471.

Conclusions

Our combined experimental and theoretical investigations demonstrate that the formation of bimetallic surfaces leads to the onset of the selective hydrogenation of the C═O bond in acrolein. More importantly, our results reveal that the structure of the bimetallic surface plays a critical role, with the subsurface Pt−Ni−Pt(111) structure being much more active and selective than the surface Ni−Pt−Pt(111) structure for the hydrogenation of the C═O bond in acrolein. The different behavior of the two bimetallic structures is explained with DFT modeling in terms of the differences in binding energies and bonding configurations of acrolein, which appear to be related to the surface d-band center of these surfaces. Such correlation in turn demonstrates the possibility to identify other bimetallic formulations and structures, on the basis of the value of the surface d-band center, that can potentially be more selective than Pt−Ni−Pt(111) for the preferential adsorption of the C═O moiety and consequently the hydrogenation of the C═O bond in acrolein and other α,β-unsaturated aldehydes.

Acknowledgment. We thank the Department of Energy, Office of Basic Energy Sciences (Grant No. DE-FG02-00ER15104), for funding. We also thank Prof. Neurock of the University of Virginia for discussion and for providing CPU time.

Supporting Information Available: Tables and a figure showing the absolute energies of hydrogen and acrolein in hartrees, optimized geometries (as Cartesian coordinates) of all DFT-calculated structures, and a top view of the adsorption structure of acrolein and H in a periodic slab containing four (3×3) unit cells to illustrate the relative positions of acrolein and H. This material is available free of charge via the Internet at http://pubs.acs.org.

JA070264M